

PHYSICAL REVIEW D

PARTICLES AND FIELDS

THIRD SERIES, VOLUME 36, NUMBER 1

1 JULY 1987

Forward charge asymmetry in 20-GeV γp reactions

V. R. O'Dell,^b P. Rankin,^k G. P. Yost,^o M. J. Harwin,^e K. Abe,^m R. Armenteros,^{k*}
T. C. Bacon,^e J. Ballam,^k H. H. Bingham,^o J. E. Brau,^q K. Braune,^k D. Brick,^b W. M. Bugg,^q
J. M. Butler,^k W. Cameron,^c H. O. Cohn,ⁱ D. C. Colley,^a G. T. Condo,^q S. Dado,^l
R. Diamond,^{d†} P. Dingus,^o P. J. Dornan,^c R. Erickson,^k R. C. Field,^k B. Franek,^j
N. Fujiwara,^h T. Glanzman,^k I. M. Godfrey,^e J. J. Goldberg,^l A. T. Goshaw,^c G. Hall,^e
E. R. Hancock,^j T. Handler,^q H. J. Hargis,^q E. L. Hart,^q K. Hasegawa,^m R. I. Hulsizer,^g
M. Jobes,^a T. Kafka,ⁿ J. F. Kent,^o G. E. Kalmus,^j D. P. Kelsey,^{*†} T. Kitagaki,^m A. Levy,^p
P. W. Lucas,^{c‡} W. A. Mann,ⁿ R. Merenyi,^{n§} R. Milburn,ⁿ C. Milstene,^p K. C. Moffeit,^k
A. Napier,ⁿ S. Noguchi,^h F. Ochiai,^f S. O'Neale,^a A. P. T. Palounek,^c I. A. Pless,^g
W. J. Robertson,^c H. Sagawa,^m T. Sato,^f J. Schneps,ⁿ S. J. Sewell,^j J. Shank,^o
A. M. Shapiro,^b R. Sugahara,^f A. Suzuki,^f K. Takahashi,^f K. Tamai,^m S. Tanaka,^m S. Tether,^g
D. A. Waide,^a W. D. Walker,^c M. Widgoff,^b C. G. Wilkins,^a S. Wolbers,^{o‡} C. A. Woods,^{e**}
A. Yamaguchi,^m R. K. Yamamoto,^g S. Yamashita,^h Y. Yoshimura,^f and H. Yuta^m

^aBirmingham University, Birmingham, England B15 2TT

^bBrown University, Providence, Rhode Island 02912

^cDuke University, Durham, North Carolina 27706

^dFlorida State University, Tallahassee, Florida 32306

^eImperial College, London, England SW7 2BZ

^fNational Laboratory for High Energy Physics (KEK), Oho-machi, Tsukuba-gun, Ibaraki 305, Japan

^gMassachusetts Institute of Technology, Cambridge, Massachusetts 02139

^hNara Womens University, Kita-uoya, Nishi-Machi Nara 630, Japan

ⁱOak Ridge National Laboratory, Oak Ridge, Tennessee 37830

^jRutherford Appleton Laboratory, Didcot, Oxon, England OX11 0QX

^kStanford Linear Accelerator Center, Stanford University, Stanford, California 94305

^lTechnion-Israel Institute of Technology, Haifa 32000, Israel

^mTohoku University, Sendai 980, Japan

ⁿTufts University, Medford, Massachusetts 02155

^oUniversity of California, Berkeley, California 94720

^pUniversity of Tel Aviv, Tel Aviv, Israel

^qUniversity of Tennessee, Knoxville, Tennessee 37916

(SLAC Hybrid Facility Photon Collaboration)

(Received 7 July 1986)

Fast forward particles photoproduced in 20-GeV interactions on a hydrogen target are shown to be preferentially positive, the asymmetry increasing with transverse momentum and Feynman x . Evidence is given that this effect is not due to forward-going target fragments. A model in which production from the photon of a forward-going spectator u is preferred over a \bar{u} , due to a higher probability for interactions of antiquarks with the proton constituents, is shown to be qualitatively consistent with the data.

INTRODUCTION

We study the forward-going charge balance (positive or negative charge excess) in inclusive photon-proton interactions. We observe a positive excess. The effect increases with increasing Feynman x (x_F) and transverse momentum (p_t), suggesting that outgoing target fragments are not

responsible. No instrumental or other biases which could explain this asymmetry were found.

Soft hadronic ($p_t \leq 1$ GeV/ c) reactions can be understood qualitatively in the light of simple quark-quark or quark-antiquark collisions without the need for more complex diagrams. For example, Ochs¹ has shown that forward-going pions in pp collisions have a momentum

distribution similar to that of u quarks in the proton. In his model the pions are formed from "spectator" quarks (those quarks not directly involved in the interaction) from the beam proton. The quarks dress without significantly modifying their original momentum. This model is complicated by the production of resonances and kinematic effects. However, the relative excess of positive or negative charge should not be sensitive to such effects. The charge balance in the forward region should depend only on the nature of the spectator quark(s).

The photon couples symmetrically to a quark-antiquark pair² which means that all kinematic distributions are the same for the quark as for the antiquark. Exact charge balance is therefore expected in the beam (photon) fragmentation region unless there are differences in the quark and antiquark interaction probabilities for collisions with target constituents. We present a model which qualitatively explains the observed charge imbalance in terms of such differences.

EXPERIMENTAL DETAILS

The data were taken with the SLAC Hybrid Facility. A linearly polarized photon beam with energy peaked at 20 GeV and a full width at half maximum of 2 GeV was incident on the SLAC 1-m bubble chamber filled with hydrogen. Downstream of the bubble chamber three stations of proportional wire chambers (PWC's), consisting of three planes each, improved the momentum determination for most charged tracks. Some identification of fast tracks (above 3.1 GeV) was made possible by the presence of two threshold Cherenkov counters, behind which was located a lead-glass wall which gave information on neutral particles and some charged particles. The downstream detectors were made insensitive around the plane containing the beam and the e^-e^+ pairs produced by photon conversions. For more details see Refs. 3-7.

Evidence either of a track in the PWC's extrapolating back to the bubble-chamber fiducial volume or of a particle depositing energy in the lead-glass wall was used to trigger the flash lamps. This gave an overall acceptance of $88 \pm 3\%$ of the hadronic cross section. The most important trigger losses are for events whose only forward-going particles occur at production angles such that they pass through the insensitive region in the downstream systems.

RESULTS

The average charge $\langle Q \rangle$ is defined by

$$\langle Q \rangle = \frac{N_+ - N_-}{N_+ + N_-},$$

where N_+ is the number of positive tracks and N_- is the number of negative tracks. We use $\langle Q \rangle$, rather than the ratio N_+/N_- , because its physical interpretation is straightforward and because its distribution will approach a Gaussian at a reasonable level of statistics, so that the errors are well understood. Early papers on this subject used a variable related to the integral charge difference.⁸ Table I is included to allow people who wish to compare our data with other data using a different variable to do so

TABLE I. Number of tracks with $p_t > 0.7$ GeV/c contributing to each x_F bin.

x_F	Number of positive tracks	Number of negative tracks	Number of events
0.0-0.1	5978	3750	7886
0.1-0.2	5232	3772	7893
0.2-0.3	4222	3396	7148
0.3-0.4	3283	2544	5645
0.4-0.5	2513	1848	4330
0.5-0.6	1793	1261	3052
0.6-0.7	1258	897	2153
0.7-0.8	756	478	1234
0.8-0.9	319	200	519
0.9-1.0	101	72	173

more easily. The inclusive $\langle Q \rangle$ distribution is plotted as a function of particle laboratory momentum (which is measured independent of particle type because of the negligible mass dependence of energy loss) in Fig. 1. The strongly positive excess in the target-fragmentation region decreases rapidly with momentum and reaches a constant average charge of about 0.1 by 5 GeV.

Figure 2(a) shows the average charge as a function of $x_F = 2p_{\parallel}/\sqrt{s}$, where \sqrt{s} is taken to be a fixed value (6.2 GeV/c²) independent of the event topology and p_{\parallel} is measured in the c.m. frame. All particles are assumed to be pions. In the forward region about 8% of all tracks are kaons but the π/K mass difference has a negligible effect on x_F for $x_F \geq 0.1$. The proton contamination dies out rapidly with increasing positive x_F ; its decreasing effect can be seen in the first few bins. No misidentified proton with a true $x_F < 0.0$ will contribute to the plot above $x_F = 0.3$. In Fig. 2(b) we repeat Fig. 2(a) restricting the sample to tracks with transverse momentum $p_t \geq 0.7$ GeV/c (open squares) and $p_t < 0.7$ GeV/c (closed circles). The high- p_t data show a distinct rise with x_F . The charge asymmetry seen in Fig. 2(b) is clearly most strongly associated with high-transverse-momentum tracks.

We have searched for possible charge-dependent biases

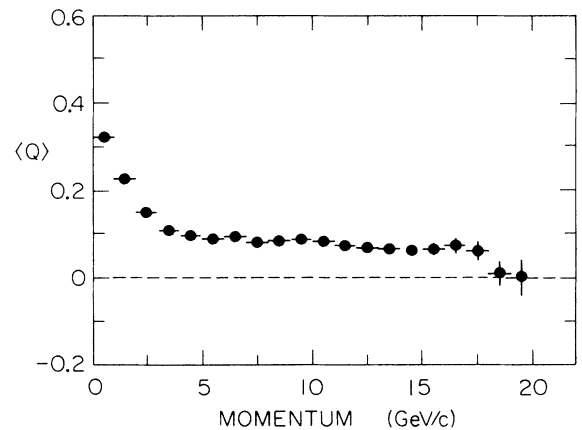


FIG. 1. The average charge $\langle Q \rangle$ as a function of particle laboratory momentum for all tracks.

in our trigger or our scanning, measuring, or reconstruction systems.

(i) The diffractive ρ^0 events provide a sample of forward particles which are well understood. The Söding⁹ model has had much success in describing the reaction $\gamma p \rightarrow \pi^+ \pi^- p$ and it includes the effect of interference terms which could cause asymmetries. A Monte Carlo calculation based on this model predicts a $\langle Q \rangle$ value consistent with zero, i.e., that the diffractive ρ^0 's will decay symmetrically, a conclusion supported by earlier data.¹⁰ In Fig. 3 we have plotted the $\pi^+ \pi^-$ invariant mass for all identified $\gamma p \rightarrow \pi^+ \pi^- p$ events showing the mass cut we used to define a ρ^0 . Figure 4 shows $\langle Q \rangle$ for the events which contain a ρ^0 , compared with the full data and the Monte Carlo calculation. We restrict the sample to tracks with $p_t \geq 0.5$ GeV/c (a lower cut than above in order to ensure adequate statistics) and we observe that the average

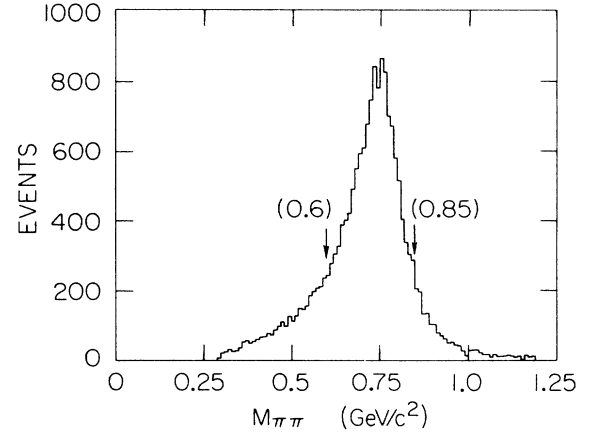


FIG. 3. The invariant mass of all identified $\gamma p \rightarrow \pi^+ \pi^- p$ events. The arrows indicate the mass cut used for extracting the $\gamma p \rightarrow \rho p$ events.

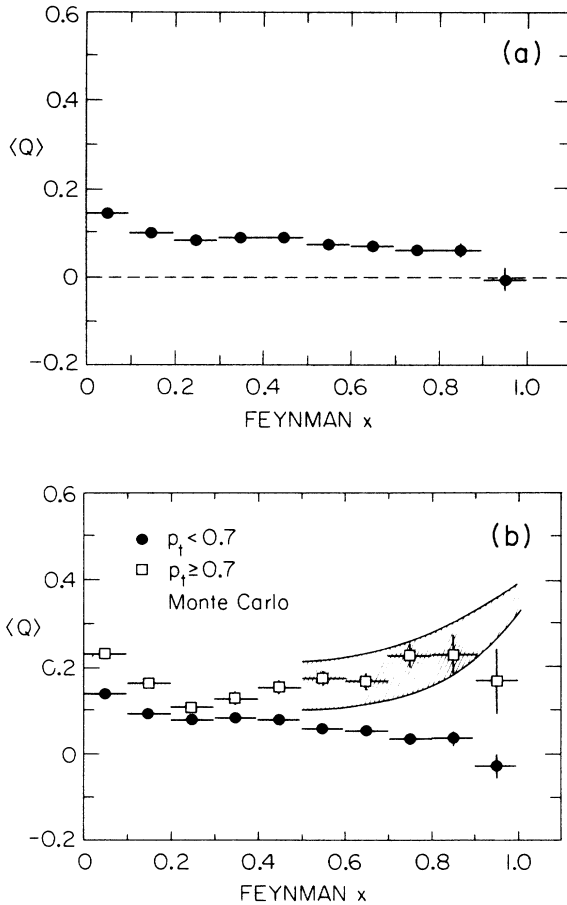


FIG. 2. Average charge plots. (a) The average charge $\langle Q \rangle$ as a function of Feynman x for all tracks. For this and all subsequent figures, all tracks measured at $x_F > 1$ (which can occur due to measurement error or the beam spread) are included in the bin 0.9 to 1.0. (b) The average charge $\langle Q \rangle$ as a function of Feynman x for all tracks with $p_t < 0.7$ GeV/c (closed circles) and for all tracks with $p_t \geq 0.7$ GeV/c (open squares). The Monte Carlo prediction is based on the annihilation model discussed in the text.

charge for the $\gamma p \rightarrow \pi^+ \pi^- p$ events is consistent with zero as the Monte Carlo calculation predicts.

(ii) A check for specific trigger biases was made by studying the events with a PWC trigger (77% of the data), and those giving a lead-glass-wall trigger (81% of the data) separately. The PWC trigger responds to charged particles only and the lead-glass-wall trigger responds to both neutral and charged particles. About 60% of all events cause both types of trigger. Figure 5 shows the charge asymmetry for these two subsets; no difference is seen between them. Similar conclusions are found from a study of events giving only a single type of trigger (not shown). Finally, a subset of the data, taken every fiftieth frame untriggered, is in agreement with the triggered data.

We conclude that there is no evidence for a trigger or

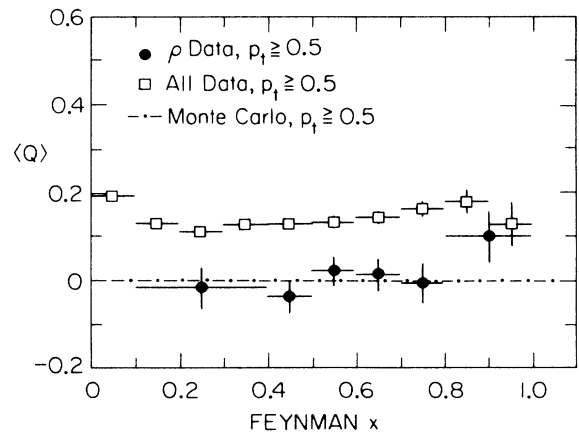


FIG. 4. The average charge $\langle Q \rangle$ as a function of Feynman x for tracks with $p_t > 0.5$ for all identified $\gamma p \rightarrow \rho p$ events (closed circles), and for all events (open squares). The Monte Carlo result uses the Söding model to predict the asymmetry for ρ events.

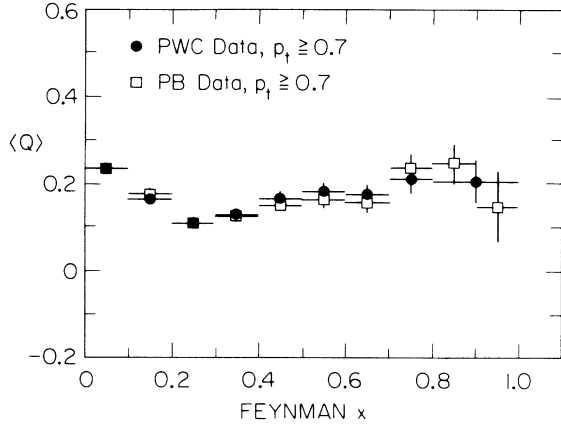


FIG. 5. The average charge $\langle Q \rangle$ as a function of Feynman x for all tracks with $p_t \geq 0.7$ GeV/c, for events which give a PWC trigger (closed circles) and for events which give a lead-glass trigger (open squares).

other experimental bias which would cause the charge asymmetry we observe.

Strange-particle production was investigated as a source of the asymmetry. There is a K^+/K^- production asymmetry, due to the fact that the associated production of K^+ and a strange baryon (predominantly Λ 's and Σ 's) is enhanced (by a factor of 30 in our experiment)¹¹ relative to K^- and a strange antibaryon. The fraction of events with a Λ has been measured to be about 5% in this experiment and the fraction of Σ^+ per event is found to be about 1%. Therefore, it would be necessary for the charge asymmetry to be very large in strange-particle events containing Λ or Σ , to account for the size of the effect we see in the full data. In Fig. 6 we show the data for events containing a visible sign of strangeness (kink or

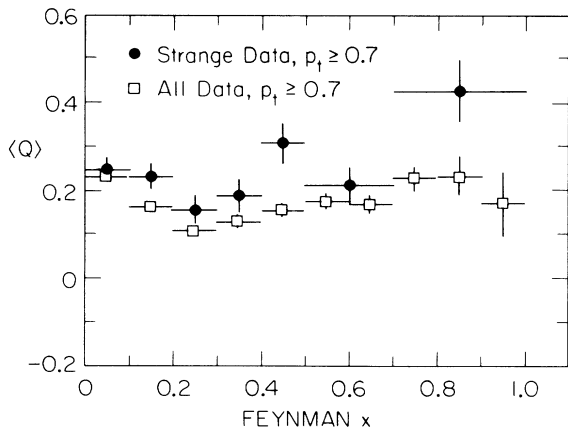


FIG. 6. The average charge $\langle Q \rangle$ as a function of Feynman x for all tracks with $p_t \geq 0.7$ GeV/c for events with a visible strange-particle topology (closed circles) and for all events (open squares).

V^0). About 50% of these are due to kaon production, about 25% to Λ production, and about 5% to Σ production. These events therefore contain a greatly enriched sample of Λ and Σ particles but do not lie enough above the full data to explain the effect. Further, removing events with visible strange-particle decays does not appreciably change the overall asymmetry. Therefore, strangeness production is not sufficient to explain the observed charge asymmetry.

COMPARISON WITH OTHER DATA

In deep-inelastic muon-proton scattering at 280 GeV/c, the European Muon Collaboration¹² (EMC) has measured a charge-asymmetry effect similar to ours. Plotting the net charge as a function of rapidity measured along the current direction, they observe a dip around a c.m. rapidity of 0.0, with a rise toward a net positive charge in the target-fragmentation direction and a smaller rise in the forward direction. They thus observe a clean separation between current and target-fragmentation regions. The data also show a rise with Bjorken x (x_{Bj}) of the net charge in the current fragmentation region. These data are consistent with a model [Fig. 7(a)] in which the ex-

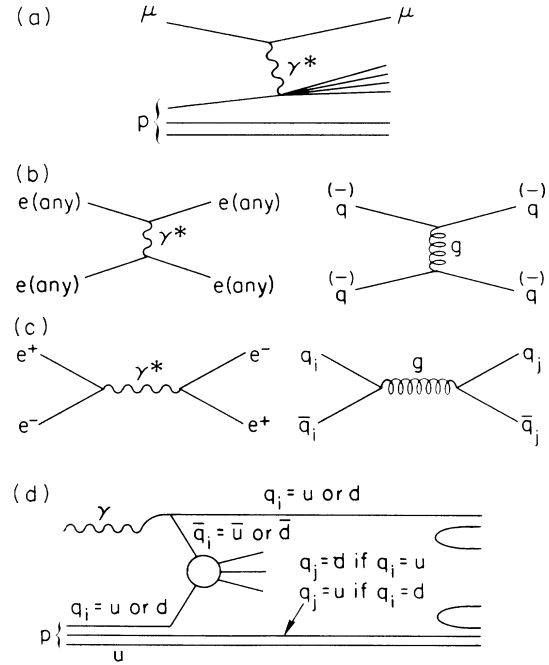


FIG. 7. Scattering diagrams. (a) Muon scattering via virtual-photon exchange. (b) t -channel scattering of electrons and/or positrons in QED and the same for quark (antiquark) scattering in QCD. (c) Annihilation diagram for e^+e^- scattering in QED and the same for quark-antiquark scattering in QCD. This channel is only open for like-flavor quark-antiquark pairs. (d) γp inclusive scattering with production of spectator quarks, showing like-flavor quark-antiquark scattering, which is favored over all other quark-antiquark and quark-quark scattering. Photon dissociation to $u\bar{u}$ is four times more likely than dissociation to $d\bar{d}$ and there are 2 u quarks to one d in the proton. The net effect is an enhanced probability of forward u spectators.

changed photon interacts as a pointlike particle with the proton constituent quarks, with probability proportional to e_q^2 (where e_q is the charge of the struck quark). Clearly, interactions with the u quark dominate, and these authors are able to account for the net positive charge in the forward direction as due to an approximate preservation of the charge of the struck quark, impelled forward.

Our experiment differs in that a real photon ($Q^2=0$) is incident. In the muoproduction data, the Q^2 is restricted to values above 4.0 GeV². For high Q^2 , the photon is thought to behave as a pointlike particle, and to interact with target quarks through a direct electromagnetic coupling. The direct coupling of a real photon to a quark (the quark Compton effect) which would favor u -quark scattering is too small at our energies to explain the effect (less than 10 nb compared to a total cross section of 120 μ b). For real photons, the vector-dominance model is known to account for at least 80% of the cross section.² In this model the photon is considered to dissociate electromagnetically into virtual charged particles, presumably quarks, which then interact. This system has actual spatial extent, and diagrams for real photon interactions involve the strong interaction between the constituents of the photon and of the target.

DISCUSSION

Buschbeck *et al.*¹³ have had considerable success in accounting for certain features of hadronic interactions with diagrams in which the annihilation of like-flavor quark-antiquark pairs enhances their interaction probability. Analogous to QED electron-positron scattering, all flavors of quarks may scatter by the t -channel exchange of a gluon [Fig. 7(b)], but only like-flavor quark-antiquark pairs have the annihilation diagram [Fig. 7(c)] open to them.

The annihilation mechanism is responsible, to first order, for the fact that the $\bar{p}p$ cross section exceeds the pp cross section up to beam energies at least as high as 50 GeV. It is also a possible mechanism for K_L - K_S regeneration, since the \bar{K}^0 contains a \bar{d} which can annihilate, unlike the K^0 . In terms of q - q or q - \bar{q} c.m. energies, 50 GeV of beam energy in $p\bar{p}$ scattering corresponds to a typical \sqrt{s} of roughly 3 or 4 GeV. Such a mechanism may explain our results [Fig. 7(d)]. Our total c.m. energy is only $\sqrt{s}=6.2$ GeV, and so the c.m. energy of any interacting partons will be low enough to be within the region of annihilation enhancement. After the photon dissociation into a $q\bar{q}$ pair the \bar{q} interacts with a larger probability than the q because of the annihilation channel, leaving the spectator q to be emitted forward more often and to dress itself into the observed forward hadrons. The probability that this spectator is a u rather than a d is enhanced because (a) the photon coupling to the $u\bar{u}$ contributes a factor of 4 in the intensity relative to the $d\bar{d}$ coupling and (b) a further factor of 2 comes from the two u quarks in the proton, either of which can annihilate. Sea $q\bar{q}$ pairs from the proton contribute only a charge-symmetric background; the sea pairs from the photon add a small amount of asymmetry. We therefore expect to observe more positive than negative charge in the far forward region, on average. Charged resonance production

should reflect this same asymmetry, and thus contribute only to a smearing of the final-state particles' x_F distributions.

We have developed a simple Monte Carlo model based on this idea.¹⁴ In our Monte Carlo model we choose a valence photon quark and a valence proton quark. We model the interactions of these quarks after pp and $p\bar{p}$ total cross sections; the probability for unlike flavors of quark-antiquark scattering or any flavors of quark-quark scattering is determined by the total pp cross section, and the probability for like flavors of quark-antiquark scattering is determined by the total $p\bar{p}$ cross section. Energy dependence is built into our Monte Carlo simulation because the pp and $p\bar{p}$ cross sections depend on \sqrt{s} . The resulting forward meson spectrum is formed by the "spectator" or noninteracting quark from the beam photon, and the meson formed by this quark is assumed (as in recombination models) to have the same x distribution as the parent quark.

The x dependences of the valence proton quarks were generated according to the following phenomenological structure functions:¹⁵

$$G_u^p(x) = 1.79(1 + 2.3x)(1-x)^3/\sqrt{x},$$

$$G_d^p(x) = 1.1(1-x)^{3.1}/\sqrt{x}.$$

It is less clear how to choose the photon structure function. Guided by generalized vector-meson dominance we may assume the photon structure function is similar to that of a meson, in which case $G_{\gamma \rightarrow q}(x) = (1-x)/\sqrt{x}$, but the quarks in the photon may be concentrated at lower x than in the pion. Several different photon structure functions of the form $G_{\gamma \rightarrow q} = (1-x)^n/\sqrt{x}$, were tried to examine the effect they have on the $\langle Q \rangle$ calculation in the Monte Carlo simulation. It was found that the form of the photon structure function does not significantly alter the result. Intuitively this is because we have chosen the same structure function for both $u\bar{u}$ and $d\bar{d}$ production. This cancels out any relative differences in "spectator" quark production as a function of x . The only difference in magnitude arises from the charge squared coupling which is independent of x and p_t .

The value we choose for the average charge of the meson formed by the spectator photon quark does affect the results of the Monte Carlo simulation. We have repeated the calculation using two different assumptions for this parameter: first that the average charge of the meson is ± 1 and second that it is the same as the charge of the spectator quark. The latter choice implies that on the average, the quark dresses itself without changing the overall charge in the photon fragmentation region. Since the fast recombining valence quark requires a sea-quark-antiquark loop to dress itself, the sea quark not used in the dressing carries an opposing charge, forming a meson which tends to compensate for the charge the recombining quark gains in the dressing. In other words the charge structure in the photon fragmentation region is not just due to the way the valence photon quark dresses itself but is also affected by how the sea quarks dress themselves.

Another important consideration is how the quarks in

the proton share their momentum. This is important when comparing the c.m. energy of the qq or $q\bar{q}$ interaction to the c.m. energy of the pp or $p\bar{p}$ interaction. If we assume that on the average all three quarks in the proton (antiproton) share the available energy equally, then we need to multiply the quark-quark c.m. energy by a factor of 3 in order to compare it to the proton-proton c.m. energy. The presence of other momentum-sharing particles in the proton (e.g., gluons) alters this calculation. Gluons may absorb as much as half of the available proton momentum, leaving the other half for the valence quarks. If we assume the valence proton quarks are allowed only half of the proton's momentum, and that they share this momentum equally, then the multiplicative factor for comparing qq c.m. energy to pp c.m. energy becomes 6.

The range of results obtained from the Monte Carlo simulation for these different assumptions is indicated on Fig. 2(b). We observe good agreement with the data.

We investigated an alternative model which crudely approximates pion exchange by altering the above Monte Carlo simulation to use total π^+p and π^-p cross sections to estimate the interaction probability of a pion exchanged between the photon and the target proton. Again different structure functions for the photon had a negligible effect on the result. Figure 8 shows $\langle Q \rangle$ vs x for the pion-exchange Monte Carlo simulation. As illustrated in the figure this Monte Carlo simulation predicts a $\langle Q \rangle$ which peaks at $x \approx 0.7$ at a value of $\langle Q \rangle \approx 0.4$. $\langle Q \rangle$ then decreases rapidly with x falling to -0.3 at $x = 1.0$. This behavior can be understood intuitively by comparing the total π^+p and π^-p cross sections. For $E_{c.m.} < 1.4$ GeV (corresponding to interacting $x_\pi < 0.2$), the π^-p cross section is smaller than the π^+p cross section, which means in the high- x region [$x \equiv 1 - x_\pi \geq 0.8$], the $\langle Q \rangle$ is dominated by spectator π^- , i.e., $\langle Q \rangle$ becomes more negative. In the region $1.4 \leq E_{c.m.} < 1.8$ GeV corresponding to $0.2 \leq x_\pi < 0.4$, the π^-p cross section is larger than the π^+p cross section leading to a positive $\langle Q \rangle$ in the region $0.6 < x < 0.8$. Similarly one can deduce the $\langle Q \rangle$ behavior in the rest of the x range. We conclude that, for our ener-

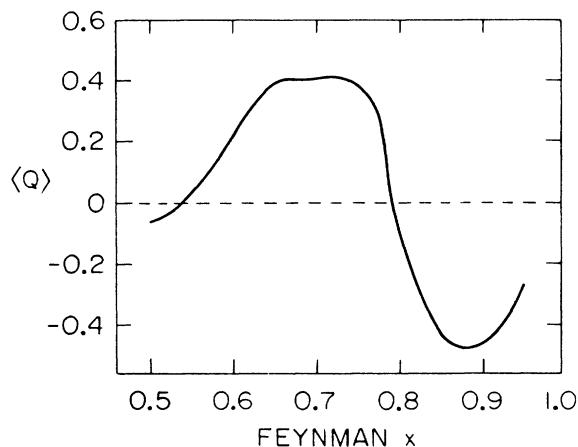


FIG. 8. The Monte Carlo prediction based on the pion-exchange model discussed in the text.

gies and assuming the exchanged pion is approximately real, this model does not fit the data, and we return to the previously discussed annihilation model.

This model implies that the effect should not be polarization dependent. We have operated in two different linear polarization modes (the polarization was about 55%) of the beam. Data taken at each polarization agree separately within errors with the full data, consistent with this model.

The model does not incorporate any p_t dependence. Possible explanations for the observed p_t dependence follow.

(1) *Low- p_t diffractive vector-meson production.* Because neutral vector mesons decay charge symmetrically, and because their pion decay products are concentrated in the low- p_t high- x region, they could be masking the charge-asymmetric structure at low p_t and high x . Only a small percentage of events ($\approx 10\%$) is identifiable as diffractive vector-meson production, however, and removing them does not appreciably enhance the charge asymmetry at low p_t , so we have concluded that the charge symmetry at low p_t is not caused purely by vector-meson production.

(2) *Quark distributions in the target.* The p_t of the spectator parton which dresses to form the observed fast-forward particle can vary, being equal and opposite to that of the interacting parton from the photon. At a given x , the higher p_t values at which the higher $\langle Q \rangle$ are observed may therefore imply a somewhat greater penetration of the interacting quark or antiquark into the proton. Translating the x distributions of the proton structure functions¹⁷ into the spatial structure of the target, we find that the gluon and sea $q\bar{q}$ distributions extend out to the largest distances, and valence quarks appear at somewhat deeper penetrations. Of these, the d quark is the most peripheral, and the u quarks tend to be more central. Very peripheral (low- p_t) collisions will therefore mostly consist of gluon and sea $q\bar{q}$ scatters which will yield charge-symmetric differential cross sections. At deeper penetrations one would expect to see a charge asymmetry because of the increasing probability of interacting off a

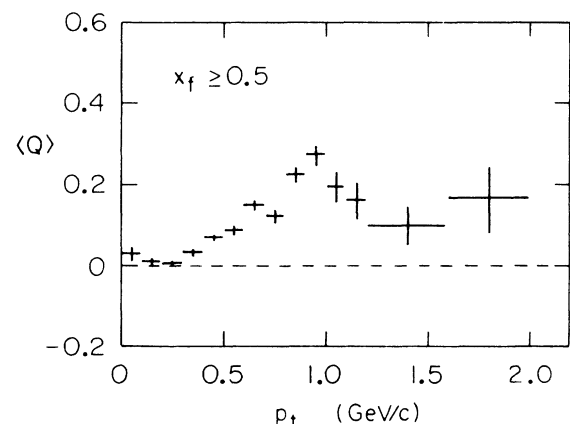


FIG. 9. The average charge $\langle Q \rangle$ as a function of p_t , the momentum of the particle transverse to the beam, for particles with $x_F > 0.5$.

valence quark, in particular a u quark as the p_t increases. This picture of deeper penetrations (higher p_t interactions) leading to increased asymmetries is qualitatively consistent with the observed behavior as a function of p_t at fixed x_F , which is shown in Fig. 9.

Experimental data for hadroproduced pions¹⁸ have been conflicting. Electroproduction experiments¹⁹ have found $\langle Q \rangle$ increasing with p_t . Therefore it seems possible that at least part of the p_t dependence of $\langle Q \rangle$ could be due to the geometry of the quarks in the target proton.

There is reasonable agreement, including the rising x_F dependence, between the model and the data, despite the model's simplicity. It establishes the plausibility of the model. The rising x_F dependence results from the fact that higher x_F spectators imply interactions at lower c.m. energies where the difference in $\sigma_{\text{tot}}(p\bar{p})$ and $\sigma_{\text{tot}}(pp)$ is more significant. This model predicts that the magnitude of the charge asymmetry should decrease with increasing energy, since the c.m. energy of parton-parton interactions will increase.

SUMMARY

In a photoproduction experiment on a hydrogen target at 20 GeV, a net positive charge is observed in the for-

ward region, which increases with both x_F and p_t . The neutral photon beam would not be expected to produce a charge asymmetry in the beam fragmentation region if its fragments are produced and dressed independently of the target. We can find no experimental bias which could cause this charge imbalance. Nor is it the result of the production of strange particles and the expected K^+/K^- asymmetry.

A mechanism involving the preferential annihilation of quark-antiquark pairs has been shown to be qualitatively consistent with the observed imbalance. This mechanism will decrease in importance with increasing photon energies.

ACKNOWLEDGMENTS

The authors would like to thank Robert Cahn, Fred Gilman, and Dave Jackson for their willingness to discuss and advise upon the physics in this paper. This work was supported in part by the Department of Energy Contract No. DE-AC03-76SF00515, the Japan-U.S. Cooperative Research Project on High Energy Physics under the Japanese Ministry of Education, Science and Culture, the UK Science and Engineering Research Council, the U.S. National Science Foundation.

*Present address: CERN, Geneva, Switzerland.

†Present address: American Dade Company, Costa Mesa, CA 92660.

‡Present address: Fermilab, P.O. Box 500, Batavia, IL 60510.

§Present address: Analytical Sciences Corporation, Reading, MA 01867.

**Present address: Langton EPS, London, England.

¹W. Ochs, Nucl. Phys. **B118**, 397 (1977).

²T. H. Bauer *et al.*, Rev. Mod. Phys. **50**, 261 (1978).

³K. Abe *et al.*, Phys. Rev. D **30**, 1 (1984).

⁴R. C. Field *et al.*, Nucl. Instrum. Methods **200**, 237 (1982).

⁵A. Bevan *et al.*, Nucl. Instrum. Methods **203**, 159 (1982).

⁶J. Brau *et al.*, Nucl. Instrum. Methods **196**, 403 (1983).

⁷J. T. Carroll in *Proceedings of the Topical Conference on Applications of Microprocessors to High Energy Physics Experiments*, Geneva, 1981 (European Organization for Nuclear Research, Geneva, 1981), p. 501.

⁸R. Erickson *et al.*, Phys. Rev. Lett. **42**, 822 (1979).

⁹P. Söding, Phys. Lett. **19**, 702 (1966).

¹⁰J. Ballam *et al.*, Phys. Rev. Lett. **24**, 960 (1970).

¹¹S. Wolbers, thesis, University of California at Berkeley, 1984;

K. Abe *et al.*, Phys. Rev. D **32**, 2869 (1985).

¹²J. P. Albanese *et al.*, Phys. Lett. **144B**, 302 (1984).

¹³B. Buschbeck *et al.*, in *Multiparticle Dynamics 1981*, proceedings of the XII International Symposium, Notre Dame, Indiana, edited by W. D. Shephard and V. P. Kenny (World Scientific, Singapore, 1982).

¹⁴V. R. O'Dell *et al.*, Report No. BC 72/73 Note:360, 1986 (unpublished).

¹⁵R. Kinnunen, University of Helsinki Report Series in Physics, Report No. HU-P-178, 1980 (unpublished).

¹⁶See, for example, J. Drees, in *Lepton and Photon Interactions at High Energies*, proceedings of the 10th International Symposium, Bonn, Germany, 1981, edited by W. Pfeil (Physikalisches Institut, Universität Bonn, Bonn, 1981), p. 474.

¹⁷See, for example, Kurt Gottfried and Victor F. Weisskopf, *Concepts of Particle Physics* (Oxford University Press, England, 1986), Chap. 5.

¹⁸I. Ajinenko *et al.*, Z. Phys. C **4**, 181 (1980); D. Brick *et al.*, *ibid.* **13**, 11 (1982).

¹⁹J. Daken *et al.*, Phys. Rev. D **10**, 1401 (1974).